JOURNAL OF COMPUTATIONAL PHYSICS 116, 39–51 (1995)

An Implicit Difference Scheme for the Long-Time Evolution of Localized Solutions of a Generalized Boussinesq System

C. I. CHRISTOV* AND G. A. MAUGIN

Laboratoire de Modélisation en Mécanique, CNRS URA 229, Université Pierre et Marie Curie (Paris VI), Tour 66, 4 Place Jussieu, boite 162, 75252 Paris Cedex 05, France

Received August 9, 1991; revised March 30, 1994

We consider the nonlinear system of equations built up from a generalized Boussinesq equation coupled with a wave equation which is a model for the one-dimensional dynamics of phases in martensitic alloys. The strongly implicit scheme employing Newton's quasilinearisation allows us to track the long time evolution of the localized solutions of the system. Two distinct classes of solutions are encountered for the pure Boussinesq equation. The first class consists of oscillatory pulses whose envelopes are localized waves. The second class consists of smoother solutions whose shapes are either heteroclinic (kinks) or homoclinic (bumps). The homoclinics decrease in amplitude with time while their support increases. An appropriate self-similar scaling is found analytically and confirmed by the direct numerical simulations to high accuracy. The rich phenomenology resulting from the coupling with the wave equation is also investigated.

I. INTRODUCTION

In recent years marked interest has developed among metallurgists, applied physicists, and mathematicians in the continuous or discrete study of changes in the structure of martensitic alloys and ferroelastic materials. In the discrete description that captures our attention in the present research, we note the works [1, 2, 3] which consider initially a lattice dynamics approach in one space dimension accounting either for the principal shear deformation alone [1] or for both shear and longitudinal deformations [3], although the latter plays a secondary role only. Further works [4, 5] account in a more satisfactory way for the material symmetry typical of the phases of these materials and various types of interparticle interactions. However, here we shall content ourselves with the model of [3] which, though less elaborate, seems to present an extremely rich dynamical behaviour.

Contrary to common models of nonlinear crystals with weak nonlocal interactions in which the classical *Boussinesq* equation for longitudinal elastic *displacement* appears to play a fundamental role ([6, pp. 5–6]), in the present case the system resulting from the continuum limit couples a *modified Boussinesq equation* for a *shear strain* to a linear wave equation for a longitudinal one. The complete system is conveniently referred to as a *generalized* Boussinesq system. The "modified" feature comes from the higher order nonlinearity needed to reproduce the typical *ferroelastic* behaviour. This obviously will be responsible for the original features to be exhibited below. These equations were shown in [3] to possess solitary wave solutions of various types that are supposed to represent several of the structures existing in real materials (solitons on austesnite and on martenite, kinks between martensitic twins). The conditions of existence of these solitary waves in terms of material parameters and their amplitude were established. Obviously, the true (in the mathematical sense) *solitonic* behaviour of these solutions could not be proved due to the very structure of the system considered here: high nonlinearity, coupling to a wave equation tantamount to producing radiation. In the present work (of which elements were briefly discussed in [7] for the case without coupling), we focus on the dynamical behaviour of the primary *discrete* system, and more particularly on the long-time evolution of traveling localized solutions developing from sharp initial data. The said problem may appear of somewhat limited significance in the original physical background as far as applications are concerned. The impact of this kind of investigation, however, can have a bearing also for different nonlinear equations of evolution.

To conduct calculations for extended times one needs a strongly implicit scheme which is stable for sufficiently large time increments. The present paper deals with devising such a scheme. In fact, the scheme proposed here is fully implicit as far as Newton's quasilinearization of the nonlinear terms is employed. The second time derivatives are approximated with second order over four time stages. The system is rendered into multidiagonal form and a specialized solver for Gaussian elimination with pivoting is used which makes the algorithm very efficient and allows us to go to very long times, indeed, with as many as 20,000 points of spatial resolution.

* Present address: Instituto Pluridisciplinar, Universidad Complutense, Paseo Juan XXIII, No. 1, Madrid 28040, Spain.

0021-9991/95 $6.00

II. POSING THE PROBLEM

Following [1, 2, 3] we consider the one-dimensional model of an atomic chain in which the longitudinal displacements x_n couple to the shear strain. Denoting the transverse displacement by y_n, the Lagrangian adopts the following form (see [3] for details).

$$\mathfrak{L} = \sum_{i=2}^{N-1} \left[\frac{m}{2}(\dot{x}_i^2 + \dot{y}_i^2) + \frac{1}{2}A(y_{i+1} - y_i)^2 - \frac{1}{4}B(y_{i+1} - y_i)^4 + \frac{1}{6}C(y_{i+1} - y_n)^6 \right] + \frac{1}{2}E(x_{i+1} - x_i)^2 - F(x_{i+1} - x_i)(y_{i+1} - y_i) + \frac{1}{2}D(y_{i+1} - 2y_i + y_{i-1})^2 \Bigg]. \tag{2.1}$$

The variables can be rendered dimensionless according to the scheme

$$L = \frac{B^3}{C^2}\mathfrak{L}, \quad \tau = \sqrt{\frac{B^2}{mc}}\,t, \quad (x_i, y_i) = \sqrt{\frac{B}{C}}\,(u_i, v_i). \tag{2.2}$$

Upon introducing the relative displacements

$$S_i \equiv v_{i+1} - v_i, \qquad T_i \equiv u_{i+1} - u_i, \tag{2.3}$$

the Euler–Lagrange equations resulting from the variation of (2.1) read

$$\begin{aligned} \ddot{S}_i = {} & c_T^2(S_{i+1} - 2S_i + S_{i+1}) - (S_{i+1}^3 - 2S_i^3 + S_{i-1}^3) \\ & + (S_{i+1}^5 - 2S_i^5 + S_{i-1}^5) \\ & - \beta(S_{i+2} - 4S_{i+1} + 6S_i - 4S_{i-1} + S_{i-2}) \\ & + (S_{i+1}^5 - 2S_i^5 + S_{i-1}^5) - 2\gamma(S_{i+1}T_{i+1} - 2S_iT_i + S_{i-1}T_{i-1}) \\ & - \beta(S_{i+2} - 4S_{i+1} + 6S_i - 4S_{i-1} + S_{i-2}), \end{aligned} \tag{2.4}$$

$$\ddot{T}_i = c_L^2(T_{i+1} - 2T_i + T_{i-1}) - \gamma(S_{i+1}^2 - 2S_i^2 + S_{i-1}^2), \tag{2.5}$$

where

$$c_T^2 = \frac{AC}{B^2}, \quad c_L^2 = \frac{EC}{B^2}, \quad \beta = \frac{DC}{B^2}, \quad \gamma = \frac{F}{B}\sqrt{\frac{C}{B}}. \tag{2.6}$$

As it is shown in [3] the continuum limit of system (2.4), (2.5) is

$$S_{tt} = c_T^2 S_{\xi\xi} - (S^3)_{\xi\xi} + (S^5)_{\xi\xi} - \alpha S_{\xi\xi\xi\xi} - \gamma(ST)_{\xi\xi}, \tag{2.7}$$

$$T_{tt} = c_L^2 T_{\xi\xi} - \gamma(S^2)_{\xi\xi}. \tag{2.8}$$

In the above system the independent space variable is defined as $\xi = X/a$ (where a is the distance between the atoms), $X_n = na$, and $\alpha = \beta - \frac{1}{2}c_T^2$ acknowledges the contribution to the fourth derivative from the respective terms of the approximation of the three-point difference $(S_{i+1} - 2S_i + S_{i-1})$. Here we mention that in terms of the longitudinal variable ξ which is scaled by the distance a, one is to keep also the higher order derivatives (sixth, eighth, etc.) in order to be consistent. Unfortunately, the resulting differential system then becomes too complicated to be tractable numerically in a feasible way. For this reason we consider in what follows either the original difference form of the system (2.4), (2.5) or a continuum limit in which the coefficient before the fourth derivative is simply β. The differential form, however, hints at the name "generalized Boussinesq system" for the system because (2.7) is a generalized Boussinesq equation in the sense of more complicated nonlinearities than the original Boussinesq equation [8].

The continuum limit can provide also the clue to how the boundary conditions are to be posed. Let us denote by ξ_1 and ξ_N the left and right boundaries of the interval under consideration, respectively. Let us consider also the physically most typical situation when the boundary points are held fixed, namely the transverse and longitudinal strains are equal to zero:

$$S = T = 0 \qquad \text{for } \xi = \xi_1, \xi_N. \tag{2.9}$$

For the discrete version of the system these boundary conditions are simply as follows

$$S_1 = S_N = T_1 = T_N = 0, \tag{2.10}$$

where the index "1" refers to the first atom in the chain and "N" to the last one, respectively.

For the transverse strain S one needs one more condition at each boundary point. The most natural condition for a strain in higher grade elasticity is

$$S_{\xi\xi} = 0 \qquad \text{for } \xi = \xi_1, \xi_N, \tag{2.11}$$

and for the proper discretization of the latter we introduce into consideration two "artificial" members of the chain with indices "0" and "$N + 1$," respectively. Then we have

$$S_0 - 2S_1 + S_2 = 0, \qquad S_{N-1} - 2S_N + S_{N+1} = 0. \tag{2.12}$$

It is clear that the very equations (2.4), (2.5) can be satisfied only at the internal points of the interval under consideration.

Before proceeding further it is important to discuss another type of boundary condition which stems from the natural boundary condition for the functional in differential form, namely

$$\frac{d}{d\xi}\left(-S^3 + S^5 - \beta\frac{d^2}{d\xi^2}S\right) = 0 \qquad \text{for } \xi = \xi_1, \xi_N. \tag{2.13}$$

The last condition is in a sense more desirable because when it is satisfied we get the following Newton law for the motion:

$$\frac{d^2}{dt^2}\int_{\xi_1}^{\xi_N} S(\xi; t)d\xi = 0. \tag{2.14}$$

Condition (2.13) is especially important when the interaction of the structures with the boundaries is investigated since it does not contribute to the total momentum of the system. We shall concern ourselves with this problem elsewhere. In the present paper we focus our attention only on localized solutions for which each of the conditions, (2.11) or (2.13), yields the other one under the provision of (2.9) due to the fact that they are asymptotic conditions imposed at infinity. We actually conducted calculations with each of the conditions, and as far as the localized solutions are concerned, we did not find a significant difference between the results.

It is interesting to note that (2.14) can provide for a conservation of the mass of a coherent structure (if any develops),

$$m(t) \equiv \int_{-\infty}^{+\infty} S(x; t)dx, \tag{2.15}$$

if the time derivative of the latter is set equal to zero at the initial moment of time. A sufficient condition for this is to require

$$\frac{d}{dt}S_i^0 = 0. \tag{2.16}$$

Then the conservation law reads

$$m(t) \equiv \text{const.} = m^0 \equiv \int_{-\infty}^{+\infty} S(x; 0)dx. \tag{2.17}$$

It is clear that depending on the magnitude of the derivative (2.16) of the initial condition one can have either a solution with linearly increasing or linearly decreasing mass or, which is the same, increasing or decreasing amplitude. The full class of localized solutions to our generalized Boussinesq system is so wide that we should confine ourselves to certain subclasses for the time being. For this reason we shall consider in what follows only solutions for which (2.16) holds.

For the successful numerical treatment of the problem of localized solutions (henceforth we call them "coherent structures") one has to consider a sufficiently large interval and hence to employ a large number of "grid points" N in order to allow enough place for the structures to move without strong interactions with other structures or with the boundaries. The second major requirement is for the temporal stability of the algorithm in the sense that the different kinds of computational errors (round-off, truncation, etc.) do not amplify timewise. The last requirement is crucial because some of the properties of the individualized localized solution can be recognized only after very long temporal evolution.

III. DIFFERENCE SCHEME AND ALGORITHM

As far as the properties of the linear system to be solved are concerned, it is better to reduce the order of the original system even at the expense of increasing the size of the system. As paradoxical as it may sound, the latter is especially important when systems with a very large number of equations are considered. This is due to the fact that the spacing h is proportional to the inverse of the size and the matrix of a system of fourth order with respect to the spatial derivatives has a determinant of order of h^4. Following this line of reasoning we introduce the auxiliary function

$$Q_i \equiv c_T^2 S_i - S_i^3 + S_i^5 - 2\gamma S_i T_i - \beta(S_{i-1} - 2S_i + S_{i+1}), \quad i = 1, ..., N-1, \tag{3.1}$$

and recast (2.4) into the form

$$\frac{d^2}{dt^2}S_i = Q_{i-1} - 2Q_i + Q_{i+1}, \qquad i = 2, ..., N-1. \tag{3.2}$$

Equation (2.5) remains unchanged,

$$\frac{d^2}{dt^2}T_i = c_L^2(T_{i-1} - 2T_i + T_{i+1}) - \gamma(S_{i-1}^2 - 2S_i^2 + S_{i+1}^2). \tag{3.3}$$

In terms of the set function Q_i, the boundary conditions adopt the simple form

$$S_1 = S_N = 0, \quad Q_1 = Q_N = 0, \quad T_1 = T_N = 0. \tag{3.4}$$

If one is to implement the boundary condition (2.16) then in terms of the function Q_i the latter adopts the following simple form:

$$Q_1 = Q_2 \qquad \text{and} \qquad Q_N = Q_{N-1}. \tag{3.5}$$

It is obvious that initial conditions are to be imposed only for functions S_i and T_i. Insofar as Eqs. (3.1) and (3.3) are of second order with respect to time, one needs two initial conditions for each of these functions, namely

$$S_i(0) = \hat{S}_i, \qquad \frac{d}{dt}S_i(0) = \tilde{S}_i, \tag{3.6}$$

$$T_i(0) = \hat{T}_i, \qquad \frac{d}{dt}T_i(0) = \tilde{T}_i. \tag{3.7}$$

In order to approximate the initial conditions to second order with respect to time we employ a staggered time mesh

$$t_n = \left(n - \frac{1}{2}\right)\tau, \tag{3.8}$$

where τ is the time increment. Introducing the superscript n to denote the current time step we derive from (3.6), (3.7) the expressions for the first two time stages $n = 0, 1$; namely,

$$S_i^0 = \hat{S}_i - \frac{\tau}{2}\tilde{S}_i, \qquad S_i^1 = \hat{S}_i + \frac{\tau}{2}\tilde{S}_i, \tag{3.9}$$

$$T_i^0 = \hat{T}_i - \frac{\tau}{2}\tilde{T}_i, \qquad T_i^1 = \hat{T}_i + \frac{\tau}{2}\hat{T}_i. \tag{3.10}$$

The main objective in devising the algorithm is to have a stable scheme that would allow us to march with large time increments τ. For this reason we chose a fully implicit scheme. At the time step $n + 1$ we use a consistent Newton's quasilinearization of the terms on the right-hand side of (3.2) and (3.3) according to the formulae:

$$S_i^3|^{n+1} = 3S_i^{n^2}S_i^{n+1} - 2S_i^{n^3} + O(\tau^2), \tag{3.11a}$$

$$S_i^5|^{n+1} = 5S_i^{n^4}S_i^{n+1} - 4S_i^{n^5} + O(\tau^2), \tag{3.11b}$$

$$S_iT_i|^{n+1} = S_i^nT_i^{n+1} + S_i^{n+1}T_i^n - S_i^nT_i^n + O(\tau^2), \tag{3.11c}$$

$$S_i^2|^{n+1} = 2S_i^nS_i^{n+1} - S_i^{n^2} + O(\tau^2). \tag{3.11d}$$

The strongly implicit scheme requires also that the time derivatives of (3.2) and (3.3) also be approximated at time step $(n + 1)$. At the first step after the two steps of the initial conditions, namely at the step numbered 2, one can have only a first-order approximation of the second derivatives over three steps:

$$\ddot{S}_i = \frac{1}{\tau^2}[S_i^2 - 2S_i^1 + S_i^0] + O(\tau), \tag{3.12a}$$

$$\ddot{T}_i = \frac{1}{\tau^2}[T_i^2 - 2T_i^1 + T_i^0] + O(\tau). \tag{3.13a}$$

At the consecutive time steps $(n > 2)$ we employ a four-step scheme with second-order approximation as follows:

$$\ddot{S}_i = \frac{1}{\tau^2}[2S_i^{n+1} - 5S_i^n + 4S_i^{n-1} - S_i^{n-2}] + O(\tau^2) \tag{3.12b}$$

$$\ddot{T}_i = \frac{1}{\tau^2}[2T_i^{n+1} - 5T_i^n + 4T_i^{n-1} - T_i^{n-2}] + O(\tau^2). \tag{3.13b}$$

Introducing the above formulas into (3.1)–(3.3), we arrive at the following *coupled* system of difference equations for the three unknown set functions S_i^{n+1}, T_i^{n+1}, and Q_i^{n+1}; namely,

$$\begin{aligned}\beta S_{i-1}^{n+1} - [2\beta + c_T^2 - 3S_i^{n^2} + 5S_i^{n^4} - 2\gamma T_i^n]S_i^{n+1} + \beta S_{i-1}^{n+1} \\ - Q_i^{n+1} + 2\gamma S_i^nT_i^{n+1} = 2S_i^{n^3} - 4S_i^{n^5} + 2\gamma S_i^nT_i^n,\end{aligned} \tag{3.14a}$$

$$Q_{i-1}^{n+1} - 2Q_i^{n+1} + Q_{i-1}^{n+1} - \frac{2}{\tau^2}S_i^{n+1} = \frac{1}{\tau^2}(-5S_i^n + 4S_i^{n-1} - S_i^{n-2}), \tag{3.14b}$$

$$\begin{aligned}c_L^2T_{i-1}^{n+1} - \left(2c_L^2 + \frac{2}{\tau^2}\right)T_i^{n+1} + c_L^2T_{i+1}^{n+1} - 2\gamma S_{i-1}^nS_{i-1}^{n+1} \\ + 4\gamma S_i^nS_i^{n+1} \\ - 2\gamma S_{i+1}^nS_{i+1}^{n+1} = \frac{1}{\tau^2}(-5T_i^n + 4T_i^{n-1} - T_i^{n-2}) \\ - \gamma(S_{i-1}^{n^2} - 2S_i^{n^2} + S_{i+1}^{n^2}).\end{aligned} \tag{3.14c}$$

Here the set functions of steps n, $n - 1$, and $n - 2$ are thought of as known. Equations (3.14) are valid for all interior points $i = 2, ..., N - 1$ and are coupled through the boundary conditions (3.4) or (3.5).

The most important feature of the system (3.4), (3.14) is that, upon introducing the composite set function

$$W_{3i-2} \equiv Q_i^{n+1}, W_{3i-1} \equiv S_i^{n+1}, W_{3i} \equiv T_i^{n+1}, \qquad i = 1, ..., N, \tag{3.15}$$

and after fairly obvious manipulations, the said system can be recast as a seven-diagonal system for the new set function W_k where $1 \leq k \leq 3N$. The band structure allows us to use highly efficient specialized solvers, e.g., the one developed in [9].

As far as we are concerned, with the localized solutions of the generalized Boussinesq system we are free to shift the independent spatial variable. This is especially important when the evolution of a structure is tracked in the moving frame. So we set the origin of the coordinate system at the point $i = N_s$. When the structure considered is symmetric (even or odd function of the spatial coordinate) then it is obvious that the best choice is $N_s = [N/2] + 1$. In each particular case the value of N_s is to be selected according to the shape of the structure in order to reduce the unnecessary calculations in that portion of the interval where the structure is virtually decayed to zero.

As we have already mentioned, the structure propagates and its "center of mass" leaves eventually the center of the coordinate system. For this reason at each time step (or after a given number of time steps, depending on the celerity with which the structure escapes the origin of the coordinate system) we calculate the actual coordinate of the center of the structure according to the formula

$$x_c = \frac{\int_{-\infty}^{+\infty} x|S^{n+1}(x;t)|\,dx}{\int_{-\infty}^{+\infty} |S^{n+1}(x;t)|\,dx}. \tag{3.16}$$

As one can see, the last formula is similar to the usual definition of the center of mass of a solitary wave save for the fact that we use the absolute value of the shape. It is because of this fact that, numerically, we are able to represent equally well both the positive and the negative parts of the shape of the solitary wave. Proceeding along these lines we calculate the new value for the index, refering to the origin of the coordinate system as

$$N_{centr} = \left[\frac{x_c}{h}\right] + N_s, \tag{3.17}$$

where h is the spacing. After that, according to (3.17) the solution is shifted in a manner to get the center of the structure once again at point N_s. This means that the value of S at point $i = N_{centr}$ should be shifted to the point $i = N_s$ and all of the remaining values accordingly. As far as localized solutions are concerned the points which remain "void" after the shifting are filled with zeros (for bump shapes) or with a given constant (for kink shapes).

To trace the evolution of a particular coherent structure one needs the flexibility to play with the scheme parameters: spacing, time increment, mesh size, actual infinity, etc. For this reason the algorithm is organized to allow one to continue from a given time stage (let us call it the "break point"), taking the result of previous calculations as an initial condition. A built-in feature of the algorithm is that during these "breaks" in the calculations one can proceed with different sets of mesh parameters. This is made possible by a procedure of spline interpolation (see [10] for details and Fortran code).

The general outline of the algorithm is as follows.

(i) The parameters for the particular run are selected and an initial condition is chosen. The computations are run without effecting the shifting procedure until a satisfactory distinguishable individual shape is formed. Then the current result is saved as disk file.

(ii) The portion of the solution whose evolution is to be traced is "cut off" from the rest and rendered in a form of initial condition. The shifting procedure is effected and the mesh parameters are adjusted if necessary. Calculations are conducted until the next break point.

(iii) At the break point the shape of the coherent structure is examined. In case it has expanded and its forerunner or its tail becomes very close to the boundaries of the computational domain an additional number of mesh points is added or some other means to enlarge the computational interval are enforced. Then the calculations are conducted until the next break point.

(iv) Step (iii) is repeated as many times as necessary in order to gather the physically relevant information of the evolution of the structure, and when this information is completed the procedure is terminated.

It is to be mentioned that if the computational boundaries are kept far enough away (see step (iii) for details) then it is not important what kinds of boundary conditions are imposed: both kinds of conditions (on the first derivative of Q or on the second derivative of S) discussed in the previous section will do if the shape is fairly decayed in the vicinity of the boundary points. This has been unequivocally confirmed by the computations.

IV. RESULTS FOR THE SOLE BOUSSINESQ EQUATION

In this section we examine the properties of our scheme for the case when the coupling is absent, i.e., $\gamma = 0$. We set $c_L = 1$, $\beta = 1$. It is easily seen that the particular values of these parameters are not as important and by selecting the value of the time increment τ we can derive most of the principal cases by means of simply rescaling the dependent and independent variables. It is stressed that, due to the strong implicitness, the scheme turns out to be stable for a wide range of time increments, $10^{-6} < \tau < 10^{6}$, and for a wide range of amplitudes of initial conditions. It is obvious that the computations with larger τ's led us to the smoother solutions spreading wider in the region under consideration.

As it has been already mentioned, we examine here only the case when the initial value for the derivative is equal to zero. Then the only freedom rests in the choice of the initial condition for the function S (for the case with coupling we define also the initial condition for function T). It is interesting to note that the particular shape of the initial condition does not matter much as far as the long-time evolution of coherent structures is concerned. After a "violent" behaviour of the solution during the first couple of time steps it eventually splits into two signals propagating in opposite directions with speed close to c_T. The most surprising observation is that when the initial condition is not symmetric then we still get two fairly similar signals but they appear to have sprung from a common origin of the coordinate system that does not coincide with the actual one. The position of this apparent origin is shifted from the real one in the direction where the amplitude of the initial condition was smaller. The initial condition is of crucial importance when the short-time evolution is of concern and especially when the boundaries of the region of consideration are not very far away. In our case they are far enough (the "actual infinity") and during the initial violent splitting of the solution into two shapes the interaction with the boundaries is negligible.

For the purposes of the exposition to follow it is enough to think of the initial condition in terms of a "difference delta function": a triangle of height C_{inl} spanning 10 points on each side of the origin of the coordinate system. In other words, the important parameter of the initial condition is its mass $m^0 = 10hC_{inl}$.

Only the smooth solutions appeared in our calculations when the time increment τ was larger than 5 regardless of the amplitude (mass) of the initial condition. It goes without saying that we did verify whether the same shape of coherent structure is obtained if the calculations are conducted with different $\tau > 5$ (say $\tau = 10$ and $\tau = 100$) and different values for the other mesh parameters, respectively. We discovered that what mattered was the interplay between the time increment and the amplitude of the initial condition. When the amplitude of the initial condition is "moderate" in comparison with τ then coherent structures with the shape of Airy functions appeared as shown in Fig. 1. It is seen that they are homoclinics. When

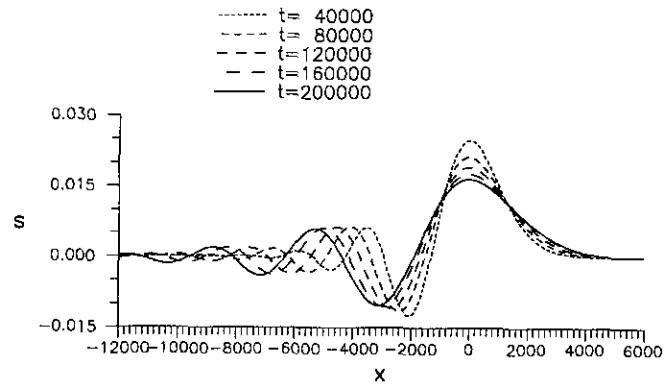

FIG. 1. Evolution with time of homoclinics of Airy-function shape: ···, $t = 4 \times 10^4$; ---, $t = 8 \times 10^4$; –––, $t = 1.2 \times 10^5$; ———, $t = 1.6 \times 10^5$; ——, $t = 2 \times 10^5$.

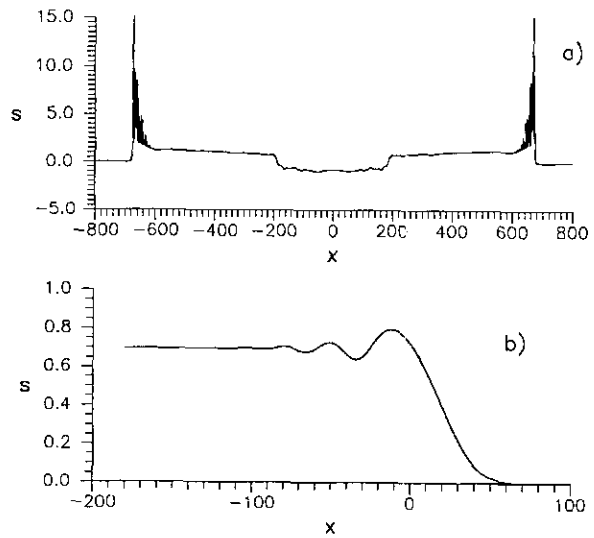

FIG. 3. The kink solution: (a) the shape of the signal at small times; (b) the shape of the kink at large times.

the amplitude is small relative to τ *the pentic nonlinearity is* switched off even on the earliest stages, and then the symmetric homoclinics shown in Fig. 2 appeared and developed steadily with time. If the amplitude was large enough, then the balance between the two nonlinear terms yielded the kink shape (heteroclinics) for the coherent structure shown in Fig. 3. Just in order to illustrate the general consequence of the computations we show in Fig. 3a the development of the initial disturbance before we cut it, say the portion of the solution to the right, and traced its evolution in the moving frame.

An interesting feature of the homoclinics is that their shape is not preserved timewise while the heteroclinics (kinks) are stationary patterns. The homoclinics appeared to be a kind of "big-bang" solution that decreased in amplitude with time while their support increased, and, after a sufficient number of time steps, the solution eventually gets on the self-similar track discussed in the next section.

A completely different universe appeared when the time increments were small enough (say $\tau < 1$ for $\beta = 1$) in order to allow development of more complicated "wiggled" shapes.

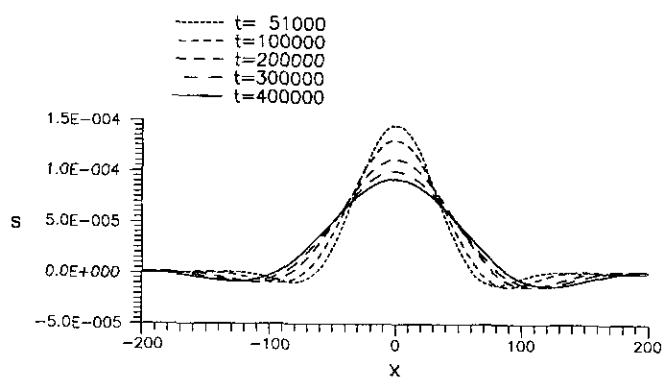

FIG. 2. Evolution with time of the homoclinics of "bump" shape: ···, $t = 5.1 \times 10^4$; ---, $t = 8 \times 10^5$; –––, $t = 2 \times 10^5$; ———, $t = 3 \times 10^5$; ——, $t = 4 \times 10^5$.

It is more convenient to consider the case $\tau = 0.1$, $\beta = 0.01$ since then the spatial span of a structure is smaller. In the sequence in Fig. 4 one sees the development of a "pulse" that has smooth shape in the right-hand side of the interval. In the course of time it spans larger portions of the left-hand side of the interval with its wavy "tail." For the time being we have not examined whether the envelope of the "pulse" exhibits some kind of self-similar behaviour as is the case with the smooth solutions.

It is mentioned here that even for small τ the large amplitudes of the initial condition led us to the kinks of Fig. 3. The complete and thorough classification and taxonomy of the different creatures inhabiting the generalized Boussinesq systems goes far beyond the scope of the present paper (which is in fact only a venture into the wild life of one of the generalized Boussinesq systems). A more systematic account is due elsewhere.

V. THE SELF SIMILAR STAGE

The results of the previous section suggest that for large times some of the solutions tend to adopt a self-similar shape in the sense that their amplitude decreases with time while the length scale of the support increases. It is instructive to check whether this is an artifact of the difference scheme (due to nonconservativeness or other shortcomings) or it is an intrinsic property of the system under consideration. Let us seek a transformation of the following type:

$$S(x;t) = \frac{1}{t^{\alpha}} s(\eta),\ T(x;t) = \frac{1}{t^{2\alpha}} \theta(\eta),\ \eta = \frac{x - ct}{t^{\delta}};\qquad \alpha, \delta > 0. \tag{5.1}$$

It is clear that for a decaying solution of the type of (5.1), for

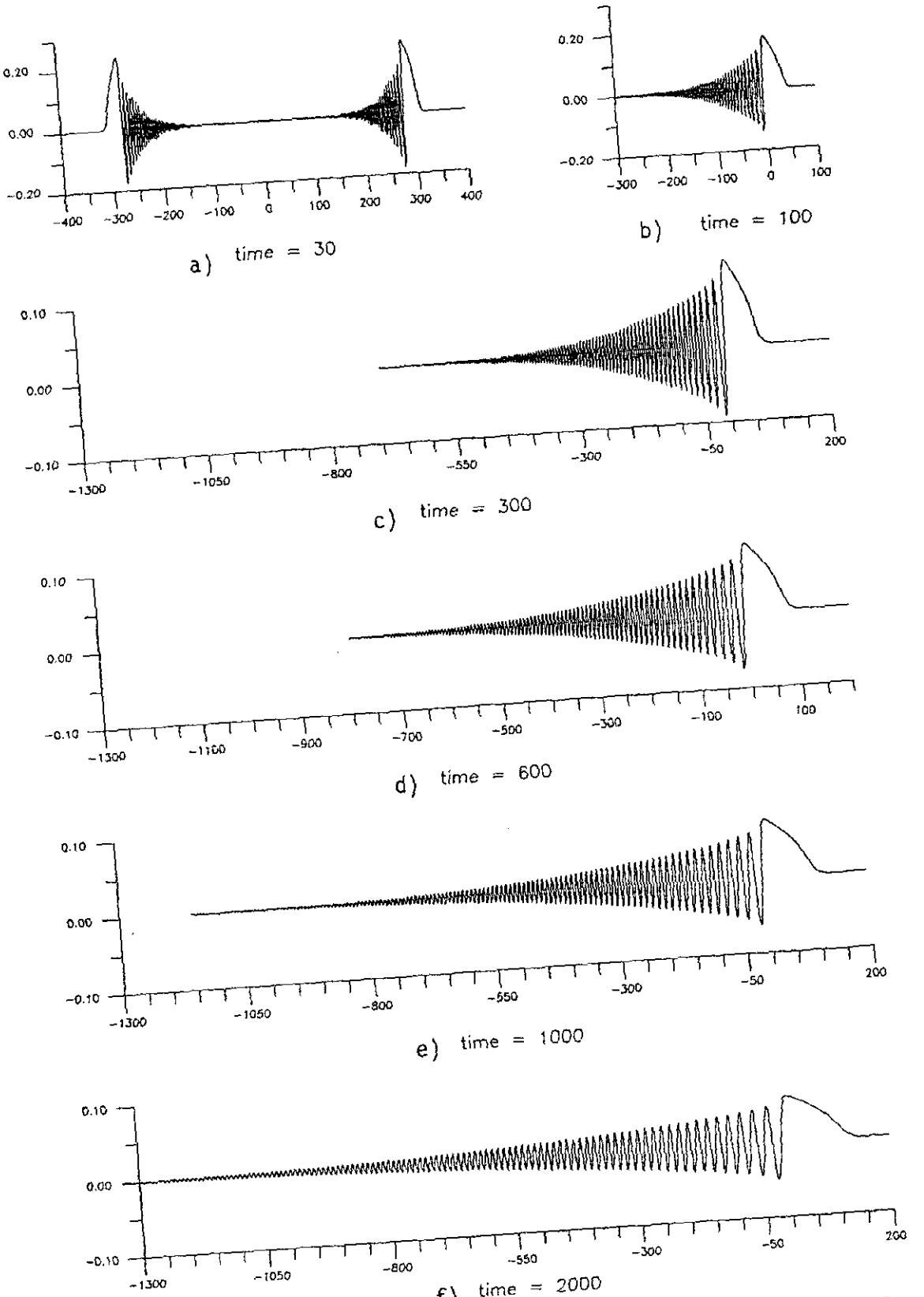

FIG. 4. The evolution of a pulse: (a) $t = 30$; (b) $t = 100$; (c) $t = 300$; (d) $t = 600$; (e) $t = 1000$; (f) $t = 2000$.

TABLE I

Self-Similar Behavior of Homoclinics of Airy-Function Shape: $t_0 = 2.76 \times 10^4$, $a = 1.011$; $b = 63.3$

Time	Amplitude	Approximation	%	Support	Approximation	%
0	0.033063	0.033445	1.1428	1866	1913.9	2.503
20000	0.027840	0.027894	0.1936	2281	2294.8	0.601
40000	0.024881	0.024818	0.2550	2587	2579.2	0.301
60000	0.022767	0.022765	0.0106	2804	2811.9	0.279
80000	0.021265	0.021257	0.0378	3002	3011.3	0.308
100000	0.020095	0.020083	0.0597	3183	3187.3	0.315
120000	0.019139	0.019132	0.0377	3343	3345.8	0.083
140000	0.018337	0.018338	0.0082	3492	3490.5	0.042
160000	0.017658	0.017662	0.0244	3632	3624.1	0.217
180000	0.017066	0.017076	0.0583	3763	3748.6	0.384
200000	0.016541	0.016560	0.1175	3884	3865.3	0.484

large times we will have $S^5 < S^3$, so the pentic power is neglected in comparison with the third one. The power law $t^{-2\alpha}$ for function T is obviously related to $t^{-\alpha}$ because of the specific form of Eqs. (2.7), (2.8). Then, introducing (5.1) into the said equations, we arrive at

$$\frac{\alpha(\alpha+1)}{t^{\alpha+2}}\frac{s}{t^{\alpha+1}}s'\left(\frac{2c_T^2}{t^\delta}+\frac{3\delta+1}{2}\frac{\eta}{t}\right) + s''\left(2c_T^2\frac{\delta\eta}{t^{1+\alpha+\delta}}+\frac{\delta^2\eta^2}{t^{\alpha+2}}\right) = \frac{1}{t^{3\alpha+2\delta}}(s^3)'' + 2\gamma\frac{1}{t^{3\alpha+2\delta}}(s\theta)'' - \frac{\beta}{t^{\alpha+4\delta}}s'''', \tag{5.2a}$$

$$\frac{\alpha(\alpha+1)}{t^{2\alpha+2}}s + \frac{2\delta+2\alpha}{t^{2\alpha+1}}s'\left(\frac{2c_L^2}{t^\delta}+\frac{3\delta+1}{2}\frac{\eta}{t}\right) + s''\left(2c_L^2\frac{\delta\eta}{t^{1+2\alpha+\delta}}+\frac{\delta^2\eta^2}{t^{2\alpha+2}}\right) = \gamma\frac{1}{t^{2\alpha+2\delta}}(s^2)''. \tag{5.2b}$$

Here primes stand for differentiation with respect to the similarity variable η.

The only way to keep the significance of the nonlinear terms at large times is to set $3\alpha + 2\delta = \alpha + 4\delta$; i.e., $\alpha = \delta$. Then the requirement of not having secular terms gives

$$\alpha = \delta = \frac{1}{3}, \tag{5.3}$$

and the final form of the equations for the scaled functions s and θ is

$$\frac{2}{3}c_T^2(4s' + \eta s'') = -(s^3)'' + 2\gamma(s\theta)'' - \beta s'''', \tag{5.4a}$$

$$\frac{2}{3}c_L^2(4\theta' + \eta\theta'') = \gamma(s^2)''. \tag{5.4b}$$

It is interesting to note that such a self-similar solution can be found both for Burgers' equation [11] and for Korteweg–de Vries' equation [6].

It goes beyond the frame of the present work to attempt a direct solution to (5.4). Rather we shall check whether the time dependent solution of the previous section conforms with the asymptotic law (5.1), (5.2). Let us confine ourselves, for the sake of simplicity, to the case without coupling, $\gamma = 0$. Let us

TABLE 2

Self-Similar Behavior of Homoclinics of Second Kind ("Bumps"): $t_0 = 7.175 \times 10^4$; $a = 0.0717$; $b = 1.473$

Time	Amplitude	Approximation	%	Support	Approximation	%
51000	0.00014591	0.00014500	0.633	83	86.23	3.750
70900	0.00013694	0.00013783	0.645	90	90.72	0.791
90000	0.00013056	0.00013212	1.179	95	94.64	0.380
150000	0.00011738	0.00011882	1.121	106	105.23	0.732
200000	0.00011032	0.00011099	0.600	113	112.66	0.303
250000	0.00010504	0.00010488	0.154	120	119.22	0.655
300000	0.00010086	0.000099926	0.935	125	125.13	0.102
400000	0.000094521	0.000092270	2.440	134	135.51	1.115

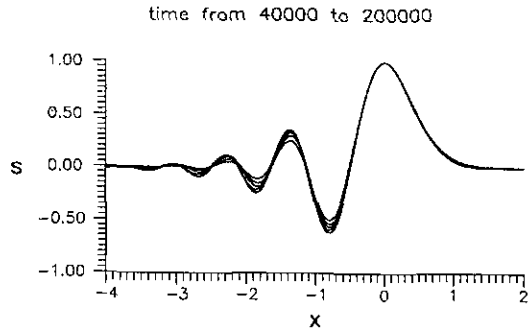

FIG. 5. Comparison of homoclinics of Airy-function shape for times from 40,000 to 200,000 after rescaling according to the self-similar law.

also define the length of support L_s as the distance from the point where the maximum of the structure is situated to the point where the amplitude is 1/100 of the maximum. The definition is appropriate for all of the structures which decay in the right portion of the region under consideration (e.g., those depicted in Figs. 1 and 2). In Tables I, II we present the amplitude and the measure of the support of the solution as functions of dimensionless time starting from a certain moment of time. Next to the column of numerical results we also present in those tables the approximation for A and L_s of the type

$$A = \frac{a}{(t + t_0)^{1/3}}, \qquad L_s = b(t + t_0)^{1/3}, \tag{5.5}$$

where the constants a, b, and t_0 are defined to provide a best fit, in the least-squares sense, to observations from numerical simulations. Here it is to be specially emphasized that the least-square functional is comprised by *both* formulas (5.5); i.e., the "imaginary" moment of time $-t_0$ is common to both formulas. Taking different α's in the two different formulas (5.5) one can even further improve the agreement, but this does not have any physical meaning. So, upon setting $x = a^3$ and $y = b^{-3}$ we cast the functional to be minimized in the form

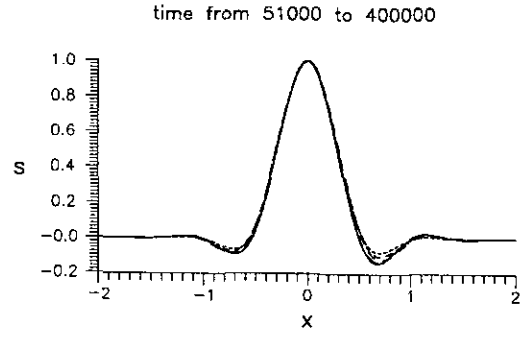

FIG. 6. Comparison of homoclinics of "bump" shape for times from 51,000 to 400,000 after rescaling according to the self-similar law.

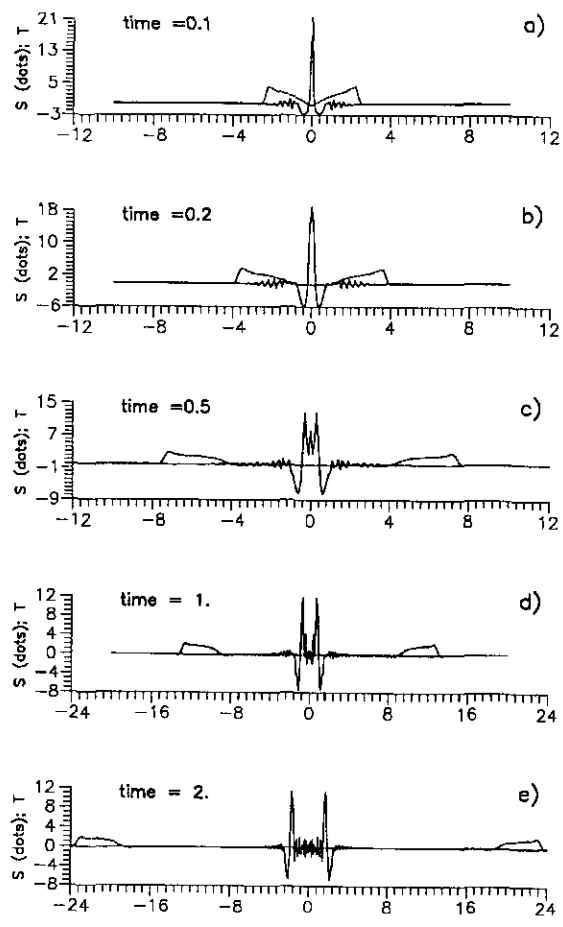

FIG. 7. Evolution of the coupled system for large starting mass $m^0 = 10.0$ and small time increment $\tau = 0.01$, $h = 0.1$, $\beta = 1$, $c_T = c_L 1$: (a) $t = 0.1$; (b) $t = 0.2$; (c) $t = 0.5$; (d) $t = 1.0$; (e) $t = 2.0$.

$$I = \sum_{k=1}^{K_t} [(A^3(t_k + t_0) - x)^2 + (L_s^{-3}(t_k + t_0) - y)^2] = \min, \tag{5.6}$$

where K_t is the total number of different time stages. It is easily seen that the problem of minimization of (5.6) reduces to solving a linear system for the three unknowns x, y, and t_0 provided that the respective sets of values for the amplitude and support are known. After the coefficients of the asymptotic law (5.5) are calculated one can "predict" the amplitude A and the support L_s and compare them to the original values in order to assess the applicability of the notion of self-similarity. This is done in Table I for the case of coherent structures of Airy-function shape. It is clearly seen that the asymptotic self-similar predictions for the amplitude A and support L_s are in excellent agreement with the observed data, the difference being less than 1% save for the moment $t = 0$ which in fact is "too early a moment" from the point of view of the asymptotic stage. The same comparison is presented in Table II but for the second kind of homoclinics ("bumps"). Although on the average the deviation here is

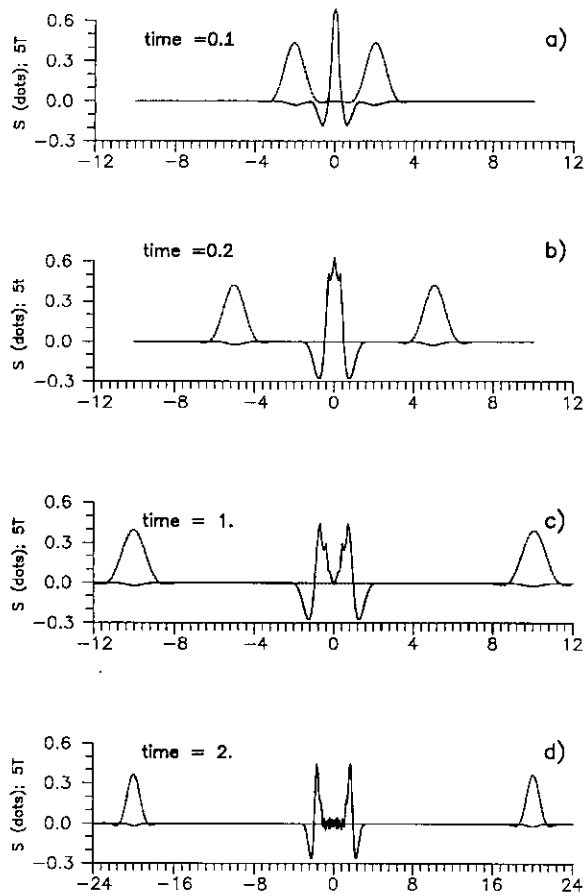

FIG. 8. Evolution of the coupled system for moderate starting mass $m^0 = 2.0$ and small time increment $\tau = 0.01$, $h = 0.1$, $\beta = 1$, $c_T = c_L 1$: (a) $t = 0.1$; (b) $t = 0.2$; (c) $t = 1.0$; (d) $t = 2.0$.

slightly larger than in the previous case, one can safely conclude that here the coherence to self-similar law is also satisfactory since the time interval is two times larger.

In Fig. 5 are shown the rescaled results for the shape of the coherent structure. One sees that the similarity is beyond any doubt. The same holds for the second kind of homoclinic solutions in Fig. 6. This means that the expanding self-similar solutions (so-called "big-bang" solutions) are an innate characteristic feature of generalized Boussinesq systems.

VI. RESULTS FOR THE COUPLED SYSTEM

As one can see from the previous sections the set of solutions of the generalized Boussinesq equation under consideration includes various different types. Its phenomenology becomes much richer when the coupling to the wave equation is acknowledged. We restrict ourselves to the case $\gamma = 1.0$ but it can be shown that by means of varying the time increment τ and rescaling the variables one can capture the main classes of behaviour of the system.

Three principal cases can be considered. The first one is when the system is excited through an initial impulse for function S and zero condition on T; the second one is the reversed situation (nontrivial initial condition for T and trivial for S); and the third is when nontrivial initial conditions are imposed for both functions. The coupling in the system under consideration is typical for interactions between the transverse and longitudinal motions in the mechanics of continua, namely the square S^2 of the transverse strain is the excitation term in the wave equation for T while the product ST plays the same role in the Boussinesq equation for S. It is obvious that if the function S is equal to zero at the initial moment, it will remain the same no matter how and to what degree we excite function T. For this reason the second case is of no interest in our study. Following the same reasoning one can show that the third case is not much different from the first one since the presence of a non-trivial initial condition for T affects the system only to the extent predetermined by the amplitude of the initial condition for S. It is to be mentioned that the algorithm presented here allowed us to impose completely different initial conditions for the two functions, and it turned out that the initial condition for the function T was important only for short initial times. Therefore, only the results relating to the first case are reported in the present section.

It is important to note that the physically encountered situation is when the speed c_L of longitudinal disturbances is larger than the speed c_T of transverse waves. The numerical experiment in this case shows that very soon a structure for function T is emitted from the main signal. This structure goes faster than the main signal and eventually separates from it. Due to the reasons discussed above the said structure does not disturb the trivial value for function S. For this reason we consider the resonant case $c_T = c_L = 1$ in order to have the structures for both functions occupying the same place in the moving coordinate system.

In Fig. 7 the evolution of the system is shown, starting from an initial condition with large mass. The dotted lines refer to the function S. As was already mentioned in Section IV the initial condition of large enough mass yields kink shapes regardless of the value of the time increment. This is clearly seen in the plots of Fig. 7 that the two structures escape from the origin of the coordinate system. What is important for the present section is the feedback to function T. The small value for time increment $\tau = 0.01$ is selected to allow development of high-frequency signals. One sees that the role of the coupling here is to give birth to an oscillatory but localized shape for function T which expands slowly timewise.

In Fig. 8 the evolution of the system is traced, with the same set of governing parameters but starting from an initial shape of smaller mass. The oscillatory bound state in the origin of the coordinate system is qualitatively the same as in the previous

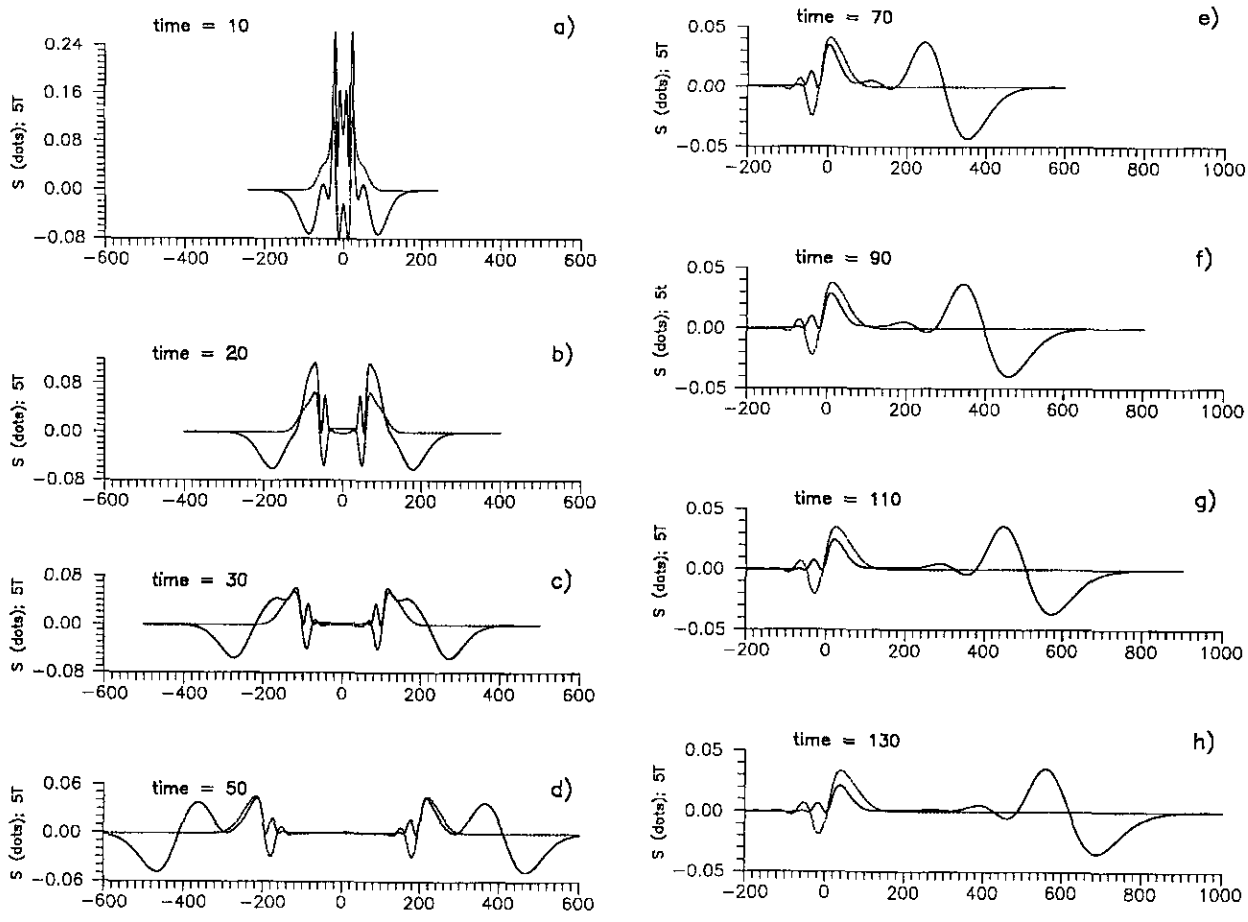

FIG. 9. Evolution of the coupled system for moderate starting mass $m^0 = 2.0$ and large time increment $\tau = 10$, $h = 2$, $\beta = 1$, $c_T = c_L = 1$: (a) $t = 10$; (b) $t = 20$; (c) $t = 30$; (d) $t = 50$; (e) $t = 70$; (f) $t = 90$; (g) $t = 110$; (h) $t = 130$.

figure. The only difference is that two "bumps" rather than kinks are escaping with the speed close to c_T.

In both Fig. 7 and Fig. 8 one can see the coupling in the smooth part of the solution (the kinks or bumps). Regarding the smooth solutions it is interesting to start the calculations with larger time increments in order to filter the oscillatory part from the very beginning and to have an unobscured picture of the evolution of the smooth solutions. The related results are presented in Figs. 9 and 10 for two different initial masses. The development of a structure of Airy-function shape is clearly seen. The said structure is "kept" in the origin of the coordinate system. What is interesting is that the overall speed of propagation of the structure is somewhat smaller than unity. This is due to the fact that the nonlinear terms contribute to some apparent celerity of the waves which causes the deviation from the linear celerity defined by c_T. That is the reason why one observes some signals for function T escaping the main signal with higher celerity. This signal is formed by part of the initial energy. Since it does not excite the function S, the effects of the nonlinearity on its celerity are not felt. As a result it is moving with phase speed equal to unity. In fact, it is the linear evolution of a structure of the wave equation. Although it is not very pronounced in Figs. 9 and 10, the apparent celerity is slightly different for the two cases shown there because it generally depends on the amplitude of solution, and the two amplitudes are different. So, referring to the main signal for which the coupling is significant, one can say that both functions S and T are of the shape of Airy function but their phases are shifted and their supports are different.

Finally, we present results for a set of parameters for which the interaction is especially strong. In this case the resonance proves to be more significant and for this reason we start in Fig. 11 with the non-resonant case $c_T = 1$, $c_L = 0.9$. Although it has little physical significance in the context of elasticity, we took the second phase speed smaller for the simple reason discussed above, namely to keep the structures for both functions in the same region. One should be aware that the actual magnitude of the function T is 10 times larger, and it is scaled in order to juxtapose it to the other function in the same figure. The feedback now is indeed mutual and one can see that the

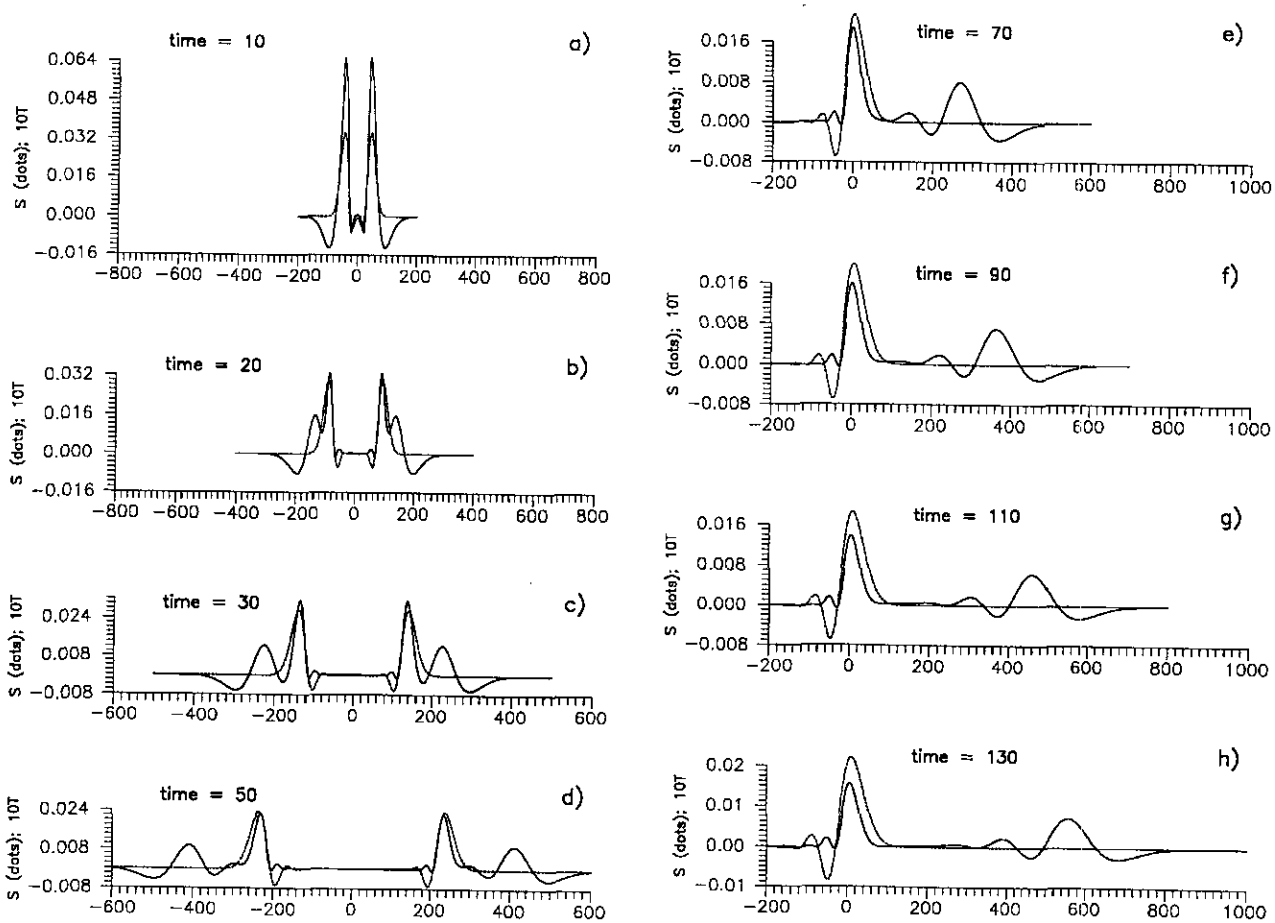

FIG. 10. Evolution of the coupled system for moderate starting mass $m^0 = 4.0$ and large time increment $\tau = 10$, $h = 2$, $\beta = 1$, $c_T = c_L = 1$: (a) $t = 10$; (b) $t = 20$; (c) $t = 30$; (d) $t = 50$; (e) $t = 70$; (f) $t = 90$; (g) $t = 110$; (h) $t = 130$.

two escaping structures of kink-like shape develop a wave forerunner which was not observed in the cases without coupling. On the other hand, the bound state around the origin of the coordinate system becomes more complicated with sharp peaks. The described behaviour of the system is grossly exaggerated by the resonance (see Fig. 12). One can think now of a stochastic shape of the signals. The last statement is applicable only in one of the halves of the interval. Otherwise, the signals are strictly (up to about four significant digits) symmetric with respect to the origin. The latter is one more validation of the algorithm discussed, bearing in mind that the calculations presented in the last two figures are conducted with 10,000 grid points.

VII. CONCLUDING REMARKS

The fully implicit difference scheme developed in the present work allowed us to follow the evolution of the localized solutions of a generalized Boussinesq system for very long times. Even this apparently narrow subclass of solutions appeared to be very rich, containing two types of homoclinics, heteroclinics, and pulses. The efficiency of the algorithm has been instrumental in discovering that the homoclinic solutions scale with the cubic root of time. The adherence of the numerical solutions to the self-similarity law is confirmed within fractions of the percent. Finally, the rich phenomenology of couplings is explored for different values of the governing parameters.

ACKNOWLEDGMENTS

The first author acknowledges a fellowship from the French Ministry of Research and Technology and partial support from Grant 1052 of the Bulgarian Ministry of Science and Higher Education.

REFERENCES

1. J. Pouget, in *Physical Properties and Thermodynamical Behaviour of Minerals*, edited by E. K. Salje, (Riedel, Dordrecht, 1988), pp. 359–401.
2. G. A. Maugin, in *Non-Classical Continuum Mechanics*, edited by R. J. Knops and A. A. Lacey, (Cambridge Univ. Press, Cambridge, 1987), pp. 272–283.

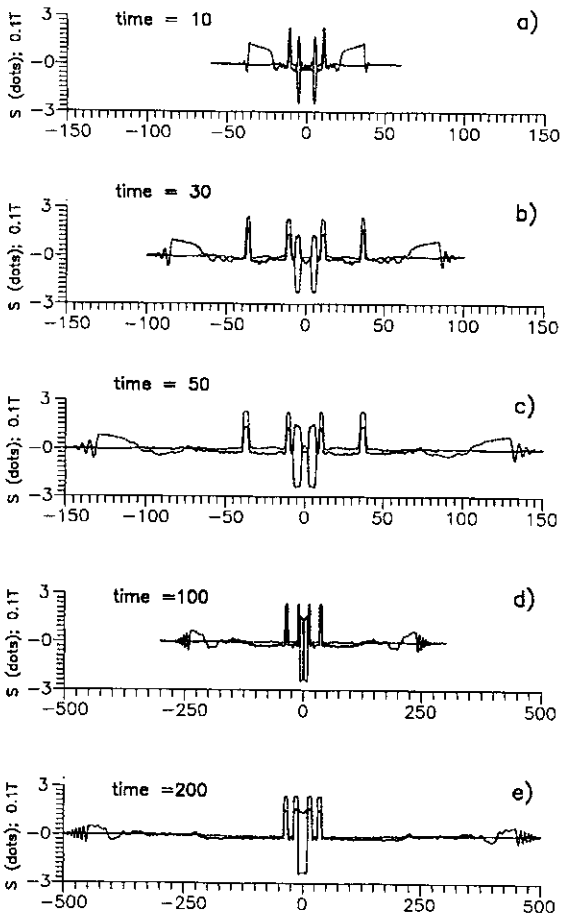

FIG. 11. Evolution of the coupled system when significant interaction is observed (non-resonant case) $m^0 = 2.5$; $\tau = 0.1$, $h = 0.5$, $\beta = 1$, $c_T = 1$, $c_L = 0.9$: (a) $t = 10$; (b) $t = 30$; (c) $t = 50$; (d) $t = 100$; (e) $t = 200$.

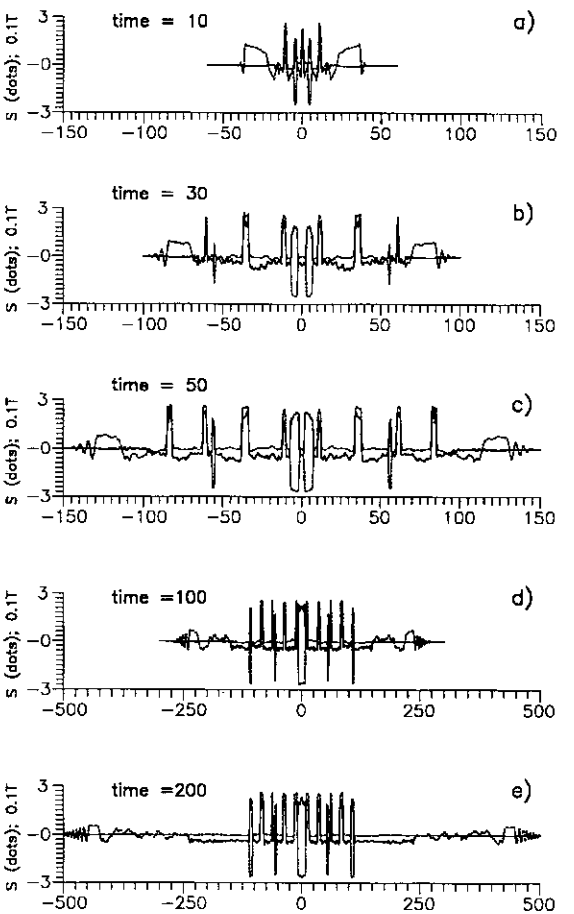

FIG. 12. Evolution of the coupled system when significant interaction is observed (resonant case) $m^0 = 2.5$; $\tau = 0.1$, $h = 0.5$, $\beta = 1$, $c_T = c_L = 1$: (a) $t = 10$; (b) $t = 20$; (c) $t = 50$; (d) $t = 100$; (e) $t = 200$.

3. G. A. Maugin and S. Cadet, *Int. J. Engng. Sci.* **29,** 243 (1991).
4. J. Pouget, in *Continuum Models and Discrete Systems,* edited by G. A. Maugin, (Longman, London, 1990), Vol. 1, pp. 296–312.
5. J. Pouget, *Phys. Rev. B* **43,** 3575 (1991).
6. A. C. Newell, *Solitons in Mathematics and Physics* (SIAM, Philadelphia, 1985).
7. J. Sander and K. Hutter, *Acta Mechanica* **86,** 111 (1991).
8. C. I. Christov and G. A. Maugin, in *Proc. 7th Interdisciplinary Workshop "Nonlinear Coherent Structures in Physics and Biology,"* edited by M. Peyrad and M. Remoissenet (Springer, New York/Berlin, 1991), pp. 209–216.
9. C. I. Christov, Gaussian elimination with pivoting for multi-diagonal systems Internal Report, University of Reading, No. 4, (1994).
10. G. E. Forsyth, M. A. Malcolm, and C. B. Moler, *Computer Methods for Mathematical Computations* (Prentice–Hall, Englewood Cliffs, NJ, 1977).
11. C. I. Christov, *Bulg. Acad. Sci., Theor. Appl. Mech.* **11,** 59 (1980) [in Russian]; see also in *Continuum Models and Discrete Systems* edited by G. A. Maugin, (Longman, London, 1990), Vol. 1, pp. 232–253.